

Enhancement of four-wave mixing via interference of multiple plasmonic conversion paths

Shailendra K. Singh,¹ M. Kurtulus Abak,^{2,3} and Mehmet Emre Tasgin^{1,*}

¹*Institute of Nuclear Sciences, Hacettepe University, 06800, Ankara, Turkey*

²*The Center for Solar Energy Research and Applications (GUNAM), Ortadoğu Teknik Üniversitesi, 06800, Ankara, Turkey*

³*Micro and Nanotechnology Program of Graduate School of Natural and Applied Sciences, Ortadoğu Teknik Üniversitesi, 06800, Ankara, Turkey*

(Received 28 July 2015; revised manuscript received 19 October 2015; published 7 January 2016)

Recent experiments demonstrate that plasmonic resonators can enhance the four-wave mixing (FWM) process by several orders of magnitude, due to the localization of the incident fields. We show that, when the plasmonic resonator is coupled to two quantum emitters, a three orders of magnitude enhancement can be obtained on top of the enhancement due to the localization. We explicitly demonstrate—on an expression for the steady-state FWM amplitude—how the presence of a Fano resonance leads to the cancellation of nonresonant terms in a FWM process. A cancellation in the denominator gives rise to an enhancement in the nonlinearity. The explicit demonstration we present here guides one to a method for achieving even larger enhancement factors by introducing additional coupling terms. The method is also applicable to Fano resonances induced by all-plasmonic couplings, which are easier to control in experiments.

DOI: [10.1103/PhysRevB.93.035410](https://doi.org/10.1103/PhysRevB.93.035410)

I. INTRODUCTION

Plasmonic resonators, such as metal nanoparticles (MNPs), graphene nanoislands [1], and transparent conducting oxides [2], confine the incident optical electromagnetic field into nanodimensions in the form of surface plasmon (SP) excitations. When a quantum emitter (QE) is placed on one of these hot spots, plasmons strongly interact with the emitter [3]. Due to the small decay rate of the QE, Fano resonances appear in the spectrum of the plasmonic material, where absorption vanishes. Fano resonances, appearing in the linear response [4], can extend the lifetime of plasmons [5,6] and lead to further enhancement of the local field [7], which makes coherent plasmon emission (spaser) possible [8].

Linear Fano resonances do not emerge only when a plasmon is coupled with a QE, but have been also observed for two interacting plasmonic materials if one has a smaller decay rate [9]. The origin of Fano resonance is analogical to electromagnetically induced transparency (EIT) [10], and can be clearly understood in terms of the interference of two absorption paths [11].

In the past decade, the role of Fano resonances in the modification of the nonlinear response has been also well studied. The presence of a quantum emitter, with an energy spacing ω_{eg} close to the output frequency, can enhance or silence the frequency conversion [12–18]. Both effects, suppression and enhancement, are desirable for devices designed to operate in linear and nonlinear regimes, respectively. The operation of high-power lasers and fiber optic cables [19] necessitates the avoidance of second harmonic generation (SHG) and Raman scattering, in order to prevent the loss of energy to other modes. On the other hand, an enhanced nonlinear response is desired for nonlinear imaging with SHG [20], four-wave mixing (FWM) [21] and Raman spectroscopy [22], and the generation of nonclassical/entangled plasmons [23].

The four-wave mixing (FWM) process—beyond its technical applications such as superresolution imaging [21], ultrafast optical switching [24,25], and nonlinear negative refraction [26]—is also important for studying one of the fundamental inquiries in quantum information. In a FWM process, two fields become entangled in addition to squeezing in one of the fields [27,28]. Hence, FWM is a special process in which the interplay between single-mode nonclassicality and two-mode entanglement coexists naturally [29]. Localization is also shown to enhance FWM in plasmonic materials [30–33] due to the larger overlap in mode integrals for that process [34,35].

Similar to SHG [14], the presence of quantum emitters attached to plasmonic converters modifies the FWM process [36–40]. Analogous to a linear response [9] and SHG [12,13,16,17], the coupling of two plasmonic materials with different decay rates creates modifications due to Fano resonances also in the FWM process [41]. Fano resonances in FWM can show themselves even as a coupling between superradiant and subradiant collective modes of plasmonic nanoclusters [40], similar to dark states in a plasmonic SHG process [42].

The presence and behavior of such resonances are well studied in the literature. In this paper, however, we demonstrate the path interference effects *explicitly* in a plasmonic FWM process. We provide a single equation [see Eq. (10)] for the steady-state amplitude of the FWM conversion. An interaction with the quantum emitter introduces extra terms in the denominator of the conversion amplitude. We show that enhancement emerges simply due to the cancellation of these extra terms with the nonresonant term in the denominator. On the contrary, conversion suppression emerges when the extra term grows several orders of magnitude—due to the small quantum decay rate—and makes the denominator blow up.

We also study the system where a plasmonic converter is coupled to two quantum emitters (QEs). We show that a better cancellation of the nonresonant term—this time also the decay term—can be achieved in the FWM process [see Eq. (14)]. FWM enhancement increases by an order of magnitude

*Corresponding author: metasgin@hacettepe.edu.tr

(15 times for the system we consider) compared to the system where the plasmonic converter is coupled with a single QE. Interestingly, we observe that the introduction of detuning for driving lasers can help the enhancement.

We present the second quantized Hamiltonian for the system of a plasmonic converter (FWM) coupled to a single quantum emitter. We obtain the equations of motion, introduce decay terms, convert operators to c numbers (since we are not interested in entanglement), and obtain the steady-state result for the converted FWM frequency [see Eq. (10)]. We repeat a similar procedure for the system of a plasmonic converter coupled to two QEs. In a previous publication, we simulated the SHG process in a coupled system using three-dimensional (3D) Maxwell equations. We compared the 3D results with the model where a classical oscillator is coupled to a QE. We observed that the presence of retardation effects in the 3D system does not significantly affect the emergence and the spectral position of the SHG enhancement (see Fig. 5 in Ref. [18]). Hence, we expect a similar effect of retardation in the present system when the dimensions of the plasmonic resonator are about 100 nm.

The model we use in this paper is shown to explain some fundamental phenomena appearing also in linear Fano resonances. As an example, it predicts (see Fig. 7 in Ref. [5]) the fluorescence enhancement of a quantum emitter coupled with a MNP [43]. It is also successful in explaining the 3D simulations of coupled (all-) plasmonic structures [17,44].

II. ORIGIN OF THE ENHANCEMENT

Hamiltonian. Nonlinear processes in plasmonic converters take place through plasmons [45] due to growing mode (overlap) integrals [34,35] with the localization. In FWM process, $\hat{a}_3^\dagger \hat{a}_2^\dagger \hat{a}_1^2 + \text{H.c.}$, the mode integral determining the strength of this process is proportional as [34]

$$\chi_{\text{FWM}} \sim \int d^3\mathbf{r} E_3^*(\mathbf{r}) E_2^*(\mathbf{r}) E_1^2(\mathbf{r}), \quad (1)$$

where E_i are the spatial extents of the electric (or polarization) fields of the \hat{a}_i plasmon modes around the nanoparticle. A nonvanishing χ_{FWM} necessitates some parity requirements for the fields of the plasmon modes, in symmetric particles.

The dynamics of the conversion process can be described as follows. The plasmonic converter has three resonances, of frequencies Ω_1 , Ω_2 , and Ω_3 , in the relevant region of the spectrum [see Fig. 1(b)]. Two lasers of frequencies ω_1 and ω_2 drive the two plasmon modes Ω_1 and Ω_2 , respectively. The lasers excite surface plasmons in the \hat{a}_1 mode (Ω_1) and \hat{a}_2 mode (Ω_2), wherein plasmons oscillate at ω_1 and ω_2 . Two plasmons in the Ω_1 mode combine and decay into two plasmons with different frequencies, one into the Ω_2 mode and another into the Ω_3 mode. The plasmon generated in the \hat{a}_3 mode (Ω_3) oscillates with frequency $\omega_3 = 2\omega_1 - \omega_2$. Decay into the Ω_2 mode is stimulated by the presence of plasmons in this mode. ω_3 plasmon oscillations emerge due to the energy conservation and the presence of a plasmon mode at $\Omega_3 \sim \omega_3$. In order to observe the ω_3 photons in the far field, plasmons in the Ω_3 mode can be selectively transformed to photons by gratings [30].

The rates of different processes, e.g., radiation damping and interband transitions, for the decay of generated FWM

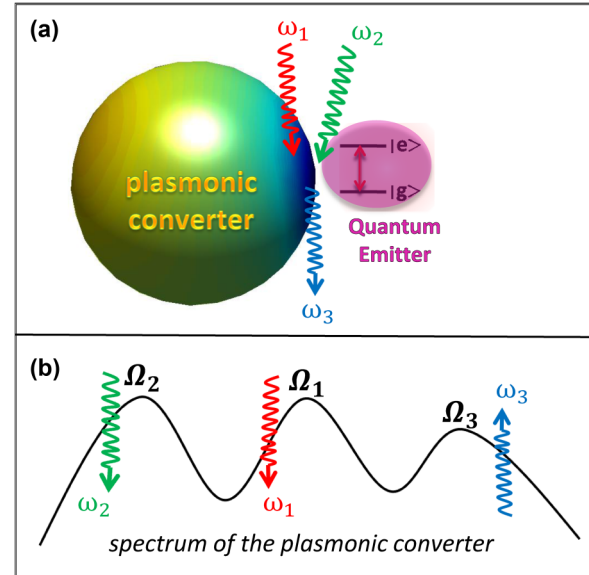


FIG. 1. (a) A quantum emitter (QE) is placed on the hot spot of a plasmonic converter. Field localization provides a strong plasmon-QE interaction. (b) Two lasers of frequencies ω_1 and ω_2 drive the plasmon modes of resonances Ω_1 and Ω_2 , respectively. Two plasmons in the Ω_1 mode, oscillating with ω_1 , combine and decay into two plasmons with different frequencies, one into the Ω_2 mode and another one into the Ω_3 mode. Decay into the Ω_2 mode is stimulated by the ω_2 laser. Frequencies are scaled with ω_1 .

plasmons may vary between different plasmonic systems (see p. 5 of Ref. [46]). This affects the number of FWM photons observed in the far field. Hence, we prefer to measure the FWM enhancement with respect to the origin [45] of the conversion process.

The Hamiltonian for the total system can be written as the sum of the energies of the quantum emitter (\hat{H}_0), plasmon modes (\hat{H}_{pls}), and the plasmon-QE interaction (\hat{H}_{int}),

$$\hat{H}_0 = \hbar\omega_e |e\rangle\langle e| + \hbar\omega_g |g\rangle\langle g|, \quad (2)$$

$$\hat{H}_{\text{pls}} = \hbar\Omega_1 \hat{a}_1^\dagger \hat{a}_1 + \hbar\Omega_2 \hat{a}_2^\dagger \hat{a}_2 + \hbar\Omega_3 \hat{a}_3^\dagger \hat{a}_3, \quad (3)$$

$$\hat{H}_{\text{int}} = \hbar(f \hat{a}_3^\dagger |g\rangle\langle e| + f^* \hat{a}_3 |e\rangle\langle g|), \quad (4)$$

including the two laser pumps (\hat{H}_{pump}) and the nonlinear FWM process (\hat{H}_{FWM}),

$$\hat{H}_p = i\hbar(\hat{a}_1^\dagger \varepsilon_p^{(1)} e^{-i\omega_1 t} + \hat{a}_2^\dagger \varepsilon_p^{(2)} e^{-i\omega_2 t} + \text{H.c.}), \quad (5)$$

$$\hat{H}_{\text{FWM}} = \hbar\chi_{\text{FWM}}(\hat{a}_3^\dagger \hat{a}_2^\dagger \hat{a}_1^2 + \hat{a}_1^\dagger \hat{a}_2 \hat{a}_3), \quad (6)$$

where f is the strength for the plasmon-QE interaction, ω_e (ω_g) is the excited (ground) state of the QE, $\varepsilon_p^{(1)}$ and $\varepsilon_p^{(2)}$ are the strengths of the two lasers of frequency ω_1 and ω_2 , and the mode integral of the nonlinear process χ_{FWM} is defined in Eq. (1). We choose the energy level spacing of the QE, $\omega_{eg} = \omega_e - \omega_g$, such that it falls into the spectral region of the Ω_3 plasmon mode. Hence, we consider the interaction of QE with the \hat{a}_3 mode only, which provides a substantial

simplification, making analytic results [Eqs. (10) and (14)] possible [47].

In Fig. 1, we depict only three plasmon modes: the two modes driven by the two strong lasers and the mode into which the FWM frequency conversion process (ω_3) takes place. In general, however, the plasmonic converter may support many modes in between Ω_1 - Ω_2 - Ω_3 or out of the region covered by these three modes. We neglect the coupling of ω_1 , ω_2 , and ω_3 excitations to other modes for the sake of obtaining a simple model. We aim at obtaining a basic physical picture. Nevertheless, such three successively placed modes can be obtained in doped graphene nanoislands [1] and by proper hybridization of two or more nanoparticles [48].

Equations of motion. The dynamics of the plasmon operators \hat{a}_i and the density operators for the QE, $\rho_{eg} = |e\rangle\langle g|$ and $\rho_{ee} = |e\rangle\langle e|$, can be obtained from the Heisenberg equation of motion, e.g., $i\hbar\dot{\hat{a}}_i = [\hat{a}_i, \hat{H}]$. We are not interested in the correlations in the system. The oscillation amplitudes (or occupation numbers) of the plasmon modes can be handled as well by replacing operators with c numbers, i.e., $\hat{a}_i \rightarrow \alpha_i$. When we introduce the plasmonic linewidths $\gamma_1, \gamma_2, \gamma_3$ and the decay rate of the quantum emitter γ_{eg} , the dynamics is governed by the coupled equations

$$\dot{\alpha}_1 = (-i\Omega_1 - \gamma_1)\alpha_1 - i2\chi_{\text{FWM}}\alpha_1^*\alpha_2\alpha_3 + \varepsilon_p^{(1)}e^{-i\omega_1 t}, \quad (7a)$$

$$\dot{\alpha}_2 = (-i\Omega_2 - \gamma_2)\alpha_2 - i\chi_{\text{FWM}}\alpha_3^*\alpha_1^2 + \varepsilon_p^{(2)}e^{-i\omega_2 t}, \quad (7b)$$

$$\dot{\alpha}_3 = (-i\Omega_3 - \gamma_3)\alpha_3 - i\chi_{\text{FWM}}\alpha_2^*\alpha_1^2 - if\rho_{ge}, \quad (7c)$$

$$\dot{\rho}_{ge} = (-i\omega_{eg} - \gamma_{eg})\rho_{ge} + if\alpha_3(\rho_{ee} - \rho_{gg}), \quad (7d)$$

$$\dot{\rho}_{ee} = -\gamma_{ee}\rho_{ee} + i(f\alpha_3^*\rho_{ge} - f^*\alpha_3\rho_{eg}), \quad (7e)$$

with $\rho_{gg} = 1 - \rho_{ee}$ and $\gamma_{ee} = 2\gamma_{eg}$.

Steady state. When the dynamics of Eqs. (7a)–(7e) is examined by placing exponential solutions, one identifies

$$\alpha_i(t) = \tilde{\alpha}_i e^{-i\omega_i t} \quad \text{and} \quad \rho_{ge} = \tilde{\rho}_{ge} e^{-i(2\omega_1 - \omega_2)t} \quad (8)$$

as the steady-state oscillations, where $\tilde{\alpha}_i$ and $\tilde{\rho}_{ge}$ are constants. It is worth noting that, in order to be confident about the validity of Eq. (8), we obtain Figs. 2 and 3 by time evolving Eqs. (7a)–(7e). When we place Eq. (8) into Eqs. (7a)–(7e), we obtain the coupled nonlinear equations

$$[i(\Omega_1 - \omega_1) + \gamma_1]\tilde{\alpha}_1 + i2\chi_{\text{FWM}}\tilde{\alpha}_1^*\tilde{\alpha}_2\tilde{\alpha}_3 = \varepsilon_p^{(1)}, \quad (9a)$$

$$[i(\Omega_2 - \omega_2) + \gamma_2]\tilde{\alpha}_2 + i\chi_{\text{FWM}}\tilde{\alpha}_3^*\tilde{\alpha}_1^2 = \varepsilon_p^{(2)}, \quad (9b)$$

$$[i(\Omega_3 + \omega_2 - 2\omega_1) + \gamma_3]\tilde{\alpha}_3 + i\chi_{\text{FWM}}\tilde{\alpha}_2^*\tilde{\alpha}_1^2 = -if\tilde{\rho}_{ge}, \quad (9c)$$

$$[i(\omega_{eg} + \omega_2 - 2\omega_1) + \gamma_{eg}]\tilde{\rho}_{ge} = if\tilde{\alpha}_3(\rho_{ee} - \rho_{gg}), \quad (9d)$$

$$\gamma_{ee}\tilde{\rho}_{ee} = i(f\tilde{\alpha}_3^*\tilde{\rho}_{ge} - f^*\tilde{\alpha}_3\tilde{\rho}_{eg}), \quad (9e)$$

for the steady-state plasmon occupations $|\tilde{\alpha}_i|^2$.

The single equation. With a simple algebraic manipulation, using Eqs. (9c) and (9d), one can reach the very simple and

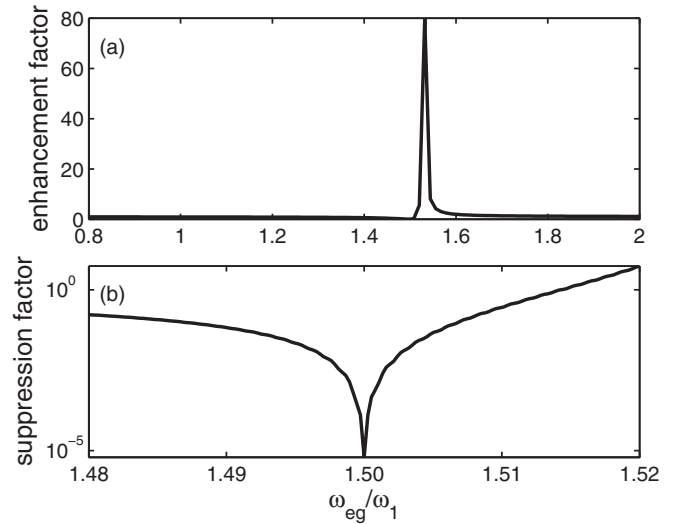


FIG. 2. (a) Relative enhancement of the FWM process in the presence of coupling to the QE, compared to a bare plasmonic converter. The first term in the denominator of Eq. (10) cancels the following nonresonant term. Such a cancellation occurs for $\omega_{eg} \simeq 1.53$ [Eq. (11)] which yields an 80 times enhancement on top of the enhancement due to field localization. (b) When $\omega_{eg} = 2\omega_1 - \omega_2 = \omega_3$, the extra term in the denominator becomes $y|f|^2/\gamma_{eg}$, which is very large and suppresses FWM.

useful equation

$$\tilde{\alpha}_3 = \frac{i\chi_{\text{FWM}}\tilde{\alpha}_2^*\tilde{\alpha}_1^2}{\frac{|f|^2 y}{[i(\omega_{eg} + \omega_2 - 2\omega_1) + \gamma_{eg}]} - [i(\Omega_3 + \omega_2 - 2\omega_1) + \gamma_3]}, \quad (10)$$

which determines the number of FWM plasmons $|\tilde{\alpha}_3|^2$, where $y = \rho_{ee} - \rho_{gg}$ is the population inversion for the QE. When coupling between the plasmonic converter and the QE is not present, $f = 0$, Eq. (10) displays the simple resonance condition for FWM. Maximum conversion is attained when

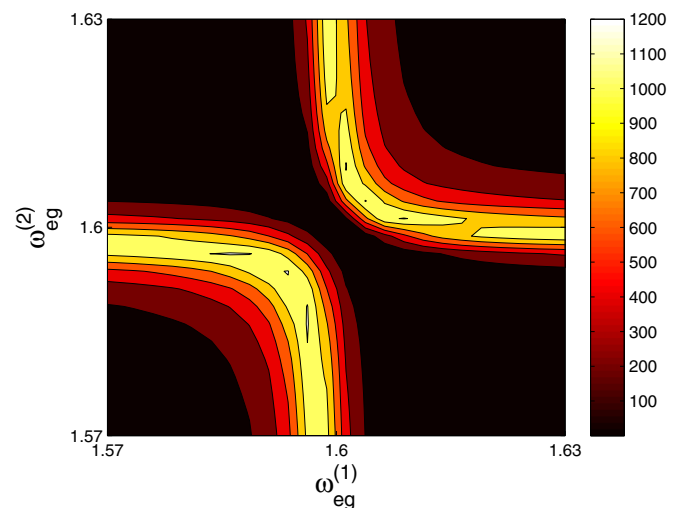


FIG. 3. When the plasmonic converter is coupled to two QEs, additional terms are introduced [see Eq. (14)]. These terms manage to partially cancel also the γ_3 term, which is not possible using a single QE as in Eq. (10). A 1200 times larger enhancement can be achieved on top of the localization enhancement.

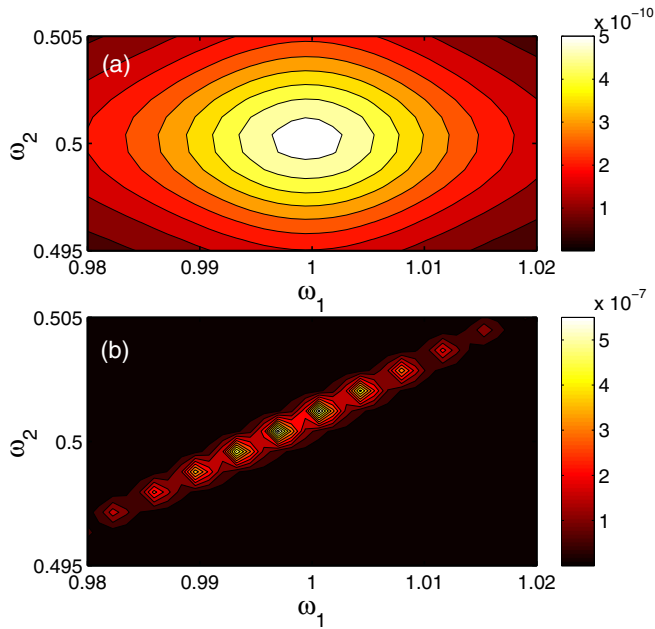


FIG. 4. Number of generated FWM plasmons, $|\tilde{\alpha}_3|^2$, for different detunings from the resonances, $\Omega_1 = 1$ and $\Omega_2 = 0.5$, of the two driving fields. (a) Spectrum of the bare plasmonic converter. (b) A single QE (of $\omega_{eg} = 1.53$) is attached to the hot spot of the converter. An enhancement factor of ~ 80 is obtained for the resonant drives $\omega_{1,2} = \Omega_{1,2}$. A larger enhancement (~ 800) at $\omega_1^* = 0.997$ and $\omega_2^* = 0.5004$ can be obtained, since ω_1 and ω_2 are involved in Eq. (10).

$2\omega_1 - \omega_2 = \Omega_3$, as should be expected. This happens when the converted frequency is resonant with the plasmon mode. In Eq. (10) we assume resonant pumping for the two lasers, $\omega_1 = \Omega_1$ and $\omega_2 = \Omega_2$, for simplicity. We refer to the term $\Omega_3 - (2\omega_1 - \omega_2)$, present in the denominator of (10), as the nonresonant term. FWM is a very weak process. Hence, one can safely consider that occupations of the two plasmon modes, $|\tilde{\alpha}_1|^2$ and $|\tilde{\alpha}_2|^2$, are almost unaffected by the conversion process. In most cases, the population stays weakly excited and one can imagine it as $y \simeq -1$.

Enhancement in FWM, in $|\tilde{\alpha}_3|^2$, can be achieved if one arranges the imaginary part of the first term of the denominator, $|f|^2 y / [i(\omega_{eg} + \omega_2 - 2\omega_1) + \gamma_{eg}]$, to cancel the nonresonant term $(\Omega_3 + \omega_2 - 2\omega_1)$. Therefore, if the level spacing of the

QE is chosen such that

$$\omega_{eg}^* = \omega_3 + \frac{|f|^2 y}{\Omega_3 - \omega_3} + \sqrt{\frac{|f|^4 y^2}{(\Omega_3 - \omega_3)^2} - 4\gamma_{eg}^2}, \quad (11)$$

then there emerges an enhancement peak in the FWM spectrum, where $\omega_3 = 2\omega_1 - \omega_2$. This is depicted in Fig. 2(a). Frequencies are scaled with ω_1 and $\omega_1 = \Omega_1 = 1$, $\omega_2 = \Omega_2 = 0.5$, $\omega_3 = 1.5$, $\Omega_3 = 1.85$, $\chi_{\text{FWM}} = 10^{-5}$, $f = 0.1$, $\gamma_1 = \gamma_2 = \gamma_3 = 0.01$, $\gamma_{eg} = 10^{-5}$. The damping rates we assign correspond to a plasmonic resonator of fair quality, $Q = 100$ [2], where quality factors of ~ 1000 are also achievable [49]. We consider a low-quality quantum dot ($\gamma_{eg} = 10^{10}/10^{15} = 10^{-5}$). The MNP-QE coupling strength f is chosen such that (i) it correctly predicts the fluorescence enhancement factor [5] in typical experiments [43] and (ii) gives rise to similar spectral results between our 3D simulations (both linear and nonlinear [18]) and the presented model. We assign a small number to the strength of the FWM process χ_{FWM} , since it is a weak process. The choice of χ_{FWM} does not affect the relative enhancement ratios as long as it is small, e.g., we checked also for $\chi_{\text{FWM}} = 10^{-12}$.

Suppression of FWM, on the contrary, can be obtained by arranging the term $|f|^2 y / [i(\omega_{eg} + \omega_2 - 2\omega_1) + \gamma_{eg}]$ to blow up. This happens when the level spacing of the QE is set to $\omega_{eg} = 2\omega_1 - \omega_2$. Since $\gamma_{eg} \sim 10^9$ Hz and plasmon resonances are typically $\sim 10^{15}$ Hz, the extra term becomes very large and leads to vanishing FWM, $|\tilde{\alpha}_3|^2$. This is depicted in Fig. 2(b).

Increasing enhancement. The enhancement in Eq. (10) is limited by the presence of γ_3 , which is not a small quantity. Hence, one naturally seeks a way to introduce extra terms to get rid of (cancel) the decay term γ_3 in the denominator. For this purpose, we consider the system where the plasmonic converter is coupled to two QEs, with strengths f_1 and f_2 . The two QEs also interact with each other with a strength g .

Hamiltonian (2)–(6) needs to be modified with additional and replacing terms

$$\hat{H}_{\text{QE-QE}} = \hbar(g|e_2\rangle\langle g_2| \otimes |g_1\rangle\langle e_1| + \text{H.c.}), \quad (12)$$

$$\hat{H}_{\text{int}} = \hbar(f_1 \hat{a}_3^\dagger |g_1\rangle\langle e_1| + f_2 \hat{a}_3^\dagger |g_2\rangle\langle e_2| + \text{H.c.}). \quad (13)$$

When the procedure, similar to Eqs. (7a)–(7e) and (9a)–(9e), is applied [50], one again obtains a single equation

$$\tilde{\alpha}_3 = \frac{i\chi_{\text{FWM}}(\beta_1\beta_2 + y_1y_2|g|^2)}{(y_1|f_1|^2\beta_2 + y_2|f_2|^2\beta_1) + iy_1y_2(f_1f_2^*g^* + f_1^*f_2g) - \xi_3(\beta_1\beta_2 + y_1y_2|g|^2)} \tilde{\alpha}_2^* \tilde{\alpha}_1^2, \quad (14)$$

where $\xi_3 = i(\Omega_3 + \omega_2 - 2\omega_1) + \gamma_3$ and $\beta_j = i(\omega_{eg}^{(j)} + \omega_2 - 2\omega_1) + \gamma_{eg}^{(j)}$ with $j = 1, 2$ enumerates QEs. Here, $\omega_{eg}^{(j)}$ and $\gamma_{eg}^{(j)}$ are the energy level spacing and the decay rate for the j th QE. y_1 and y_2 are population inversions.

This time, the extra terms cancel γ_3 more efficiently. In Fig. 3, we see that the cancellation in the denominator [Eq. (14)] results in a 1200 times enhancement for FWM, which is 15 times larger compared to the one for a single QE [Eq. (10)]. In order to maximize $\tilde{\alpha}_3$ in Eq. (14), we numerically minimize the denominator by varying f_1 , f_2 , g ,

$\omega_{eg}^{(1)}$, and $\omega_{eg}^{(2)}$ [50]. In principle, the desired phase for the QE-QE interaction (g) or plasmon-QE interactions ($f_{1,2}$) can be obtained by arranging the phase of the interaction integral [34,35] by reshaping the two QEs. In the case of all-plasmonic Fano resonances [13,15], such an arrangement among the interacting plasmon modes would be much simpler.

Spectrum of the enhancement. In deriving Eqs. (10) and (14), we assumed resonant pumping of the two modes, i.e., $\omega_{1,2} = \Omega_{1,2}$. However, in Eq. (10) we see that ω_1 and ω_2 appear in the interfering terms. In Fig. 4, we plot the spectrum

for the FWM enhancement. We see that the denominator of Eq. (10) can be minimized by varying the two driving (laser) frequencies from their resonance. The spectral position where maximum enhancement (~ 800) is attained is for $\omega_1^* = 0.997$ and $\omega_2^* = 0.5004$. For the resonant drives, $\omega_{1,2} = \Omega_{1,2}$, we observe the ~ 80 enhancement factor as in Fig. 2.

Role of path interference. Both linear and nonlinear plasmonic path interference effects are semiclassical analogs of EIT [10,51,52] which emerges in multilevel atoms. The major difference in the plasmonic systems, compared to the EIT ones, is they do not necessitate an auxiliary microwave field. The weak hybridization in the excited plasmon mode is induced by the coupling of the plasmon polarization with the attached molecule. Two unresolved modes rely on the spectral width of the plasmon mode [11]. In the nonlinear case, a molecule introduces two conversion paths, both relying on the extent of the Ω_3 mode. In the FWM process, the converted frequency is forced to emerge into the Ω_3 mode due to energy conservation. When ω_{eg} is set to ω_3 , the conversions of the two paths interfere destructively. When ω_3 is arranged appropriately, the two paths (dressed in the language of EIT) interfere constructively [51,52], similar to the EIT case. Hence, an enhancement of conversion takes place. Since such path interference effects emerge also in full-plasmonic systems [15,44] with long-lived dark modes, an adoption to these systems is possible.

III. CONCLUSION

We obtain the steady-state amplitude of the FWM process as a single equation for a plasmonic converter coupled to quantum emitters (QEs). The denominator of this equation

explicitly reveals the path interference effects. The presence of QEs, interacting with the plasmonic converter, introduces extra terms in the denominator. When the extra terms cancel the nonresonant term for the conversion, an enhancement of FWM is observed. Contrarily, when the extra term blows up due to the long lifetime of the QE, suppression of FWM is observed.

We utilize this observation as a tool for obtaining a larger enhancement in FWM. We show that, for the coupling of the plasmonic converter to two QEs, a better cancellation of the denominator is achieved. Enhancement increases by a factor of 15 on top of the resonance obtained by coupling with a single QE. Hence, an extra three orders enhancement factor emerges on top of the enhancement due to localization effects. We also examine the spectrum of the enhancement with respect to both driving (laser) frequencies. We observe that introducing detuning in the drives can help the FWM enhancement.

Fano resonances, both in the linear and nonlinear response, emerge also by coupling the plasmonic converter with a plasmonic material which has a smaller decay rate [13,15–17]. Hence, it is possible to generalize our method [44] to interacting plasmonic clusters, since the experiments are easier to conduct with nanoparticles.

ACKNOWLEDGMENTS

M.E.T. and S.K.S. acknowledge support from TÜBİTAK-1001 Grant No. 114F170. M.K.A. acknowledges support from TÜBİTAK-1001 Grant No. 113F239.

-
- [1] J. D. Cox and F. J. G. de Abajo, Plasmon-enhanced nonlinear wave mixing in nanostructured graphene, *ACS Photonics* **2**, 306 (2015).
 - [2] P. R. West, S. Ishii, G. V. Naik, N. K. Emani, V. M. Shalaev, and A. Boltasseva, Searching for better plasmonic materials, *Laser Photonics Rev.* **4**, 795 (2010).
 - [3] A. G. Curto, G. Volpe, T. H. Taminiau, M. P. Kreuzer, R. Quidant, and N. F. van Hulst, Unidirectional emission of a quantum dot to a nanoantenna, *Science* **329**, 930 (2010).
 - [4] A. Manjavacas, J. García de Abajo, and P. Nordlander, Quantum plexcitonics: Strongly interacting plasmons and excitons, *Nano Lett.* **11**, 2318 (2011).
 - [5] M. E. Taşgın, Metal nanoparticle plasmons operating within a quantum lifetime, *Nanoscale* **5**, 8616 (2013).
 - [6] S. M. Sadeghi, W. J. Wing, and R. R. Gutha, Undamped ultrafast pulsation of plasmonic fields via coherent exciton-plasmon coupling, *Nanotechnology* **26**, 085202 (2015).
 - [7] B. Lukyanchuk, N. I. Zheludev, S. A. Maier, N. J. Halas, P. Nordlander, H. Giessen, and C. T. Chong, The Fano resonance in plasmonic nanostructures and metamaterials, *Nat. Mater.* **9**, 707 (2010).
 - [8] M. A. Noginov, G. Zhu, A. M. Belgrave, R. Bakker, V. M. Shalaev, E. E. Narimanov, S. Stout, E. Herz, T. Suteewong, and U. Wiesner, Demonstration of a spaser-based nanolaser, *Nature (London)* **460**, 1110 (2009).
 - [9] P. Tassin, L. Zhang, R. Zhao, A. Jain, T. Koschny, and C. M. Soukoulis, Low-Loss Metamaterials Based on Classical Electromagnetically Induced Transparency, *Phys. Rev. Lett.* **109**, 187401 (2012).
 - [10] M. O. Scully and M. S. Zubairy, *Quantum Optics* (Cambridge University Press, Cambridge, U.K., 1997).
 - [11] C. L. G. Alzar, M. A. G. Martinez, and P. Nussenzveig, Classical analog of electromagnetically induced transparency, *Am. J. Phys.* **70**, 37 (2002).
 - [12] G. F. Walsh and L. Dal Negro, Enhanced second harmonic generation by photonic-plasmonic Fano-type coupling in nanoplasmonic arrays, *Nano Lett.* **13**, 3111 (2013).
 - [13] J. Berthelot, G. Bachelier, M. Song, P. Rai, G. C. des Francs, A. Dereux, and A. Bouhelier, Silencing and enhancement of second-harmonic generation in optical gap antennas, *Opt. Express* **20**, 10498 (2012).
 - [14] H. A. Clark, P. J. Campagnola, J. P. Wuskell, A. Lewis, and L. M. Loew, Second harmonic generation properties of fluorescent polymer-encapsulated gold nanoparticles, *J. Am. Chem. Soc.* **122**, 10234 (2000).
 - [15] K. Thyagarajan, J. Butet, and O. J. F. Martin, Augmenting second harmonic generation using Fano resonances in plasmonic systems, *Nano Lett.* **13**, 1847 (2013).
 - [16] J. Butet, G. Bachelier, I. Russier-Antoine, F. Bertorelle, A. Mosset, N. Lascoux, C. Jonin, E. Benichou, and P.-F. Brevet,

- Nonlinear Fano profiles in the optical second-harmonic generation from silver nanoparticles, *Phys. Rev. B* **86**, 075430 (2012).
- [17] J. Butet and O. J. F. Martin, Fano resonances in the nonlinear optical response of coupled plasmonic nanostructures, *Opt. Express* **22**, 29693 (2014).
- [18] D. Turkpence, G. B. Akguc, A. Bek, and M. E. Tasgin, Engineering nonlinear response of nanomaterials using Fano resonances, *J. Opt.* **16**, 105009 (2014).
- [19] A. R. Chraplyvy, Limitations on lightwave communications imposed by optical-fiber nonlinearities, *J. Lightwave Technol.* **8**, 1548 (1990).
- [20] P. Pantazis, J. Maloney, D. Wu, and S. E. Fraser, Second harmonic generating (SHG) nanoprobles for in vivo imaging, *Proc. Natl. Acad. Sci. USA* **107**, 14535 (2010).
- [21] B. Simkhovich and G. Bartal, Plasmon-Enhanced Four-Wave Mixing for Superresolution Applications, *Phys. Rev. Lett.* **112**, 056802 (2014).
- [22] B. Sharma, R. R. Frontiera, A. I. Henry, E. Ringe, and R. P. Van Duyne, SERS: Materials, applications, and the future, *Mater. Today* **15**, 16 (2012).
- [23] E. Altevischer, M. P. van Exter, and J. P. Woerdman, Plasmon-assisted transmission of entangled photons, *Nature (London)* **418**, 304 (2002).
- [24] N. Rotenberg, M. Betz, and H. M. van Driel, Ultrafast All-Optical Coupling of Light to Surface Plasmon Polaritons on Plain Metal Surfaces, *Phys. Rev. Lett.* **105**, 017402 (2010).
- [25] M. Kauranen and A. V. Zayats, Nonlinear plasmonics, *Nat. Photonics* **6**, 737 (2012).
- [26] S. Palomba, S. Zhang, Y. Park, G. Bartal, X. Yin, and X. Zhang, Optical negative refraction by four-wave mixing in thin metallic nanostructures, *Nat. Mater.* **11**, 34 (2012).
- [27] C. Genes and P. R. Berman, Atomic entanglement generation with reduced decoherence via four-wave mixing, *Phys. Rev. A* **73**, 063828 (2006).
- [28] Y. Fang and J. Jing, Quantum squeezing and entanglement from a two-mode phase-sensitive amplifier via four-wave mixing in rubidium vapor, *New J. Phys.* **17**, 023027 (2015).
- [29] J. K. Asboth, J. Calsamiglia, and H. Ritsch, Computable Measure of Nonclassicality for Light, *Phys. Rev. Lett.* **94**, 173602 (2005); W. Vogel and J. Sperling, Unified quantification of nonclassicality and entanglement, *Phys. Rev. A* **89**, 052302 (2014); W. Ge, M. E. Tasgin, and M. S. Zubairy, Conservation relation of nonclassicality and entanglement of Gaussian states in a beam splitter, *ibid.* **92**, 052328 (2015).
- [30] J. Renger, R. Quidant, N. van Hulst, S. Palomba, and L. Novotny, Free-Space Excitation of Propagating Surface Plasmon Polaritons by Nonlinear Four-Wave Mixing, *Phys. Rev. Lett.* **103**, 266802 (2009).
- [31] S. Palomba and L. Novotny, Nonlinear Excitation of Surface Plasmon Polaritons by Four-Wave Mixing, *Phys. Rev. Lett.* **101**, 056802 (2008).
- [32] J. Renger, R. Quidant, N. van Hulst, and L. Novotny, Surface-Enhanced Nonlinear Four-Wave Mixing, *Phys. Rev. Lett.* **104**, 046803 (2010).
- [33] G. I. Stegeman, J. J. Burke, and D. G. Hall, Nonlinear optics of long range surface plasmons, *Appl. Phys. Lett.* **41**, 906 (1982)
- [34] P. Ginzburg, A. Krasavin, Y. Sonnefraud, A. Murphy, R. J. Pollard, S. A. Maier, and A. V. Zayats, Nonlinearly coupled localized plasmon resonances: Resonant second-harmonic generation, *Phys. Rev. B* **86**, 085422 (2012).
- [35] M. Finazzi and F. Ciccacci, Plasmon-photon interaction in metal nanoparticles: Second-quantization perturbative approach, *Phys. Rev. B* **86**, 035428 (2012).
- [36] E. Paspalakis, S. Evangelou, S. G. Kosionis, and A. F. Terzis, Strongly modified four-wave mixing in a coupled semiconductor quantum dot-metal nanoparticle system, *J. Appl. Phys.* **115**, 083106 (2014).
- [37] Z. Lu and K.-D. Zhu, Enhancing Kerr nonlinearity of a strongly coupled exciton-plasmon in hybrid nanocrystal molecules, *J. Phys. B* **41**, 185503 (2008).
- [38] S. Evangelou, V. Yannopapas, and E. Paspalakis, Modification of Kerr nonlinearity in a four-level quantum system near a plasmonic nanostructure, *J. Mod. Opt.* **61**, 1458 (2014).
- [39] J.-B. Li, N.-C. Kim, M.-T. Cheng, L. Zhou, Z.-H. Hao, and Q.-Q. Wang, Optical bistability and nonlinearity of coherently coupled exciton-plasmon systems, *Opt. Express* **20**, 1856 (2012).
- [40] Y. Zhang, F. Wen, Y.-R. Zhen, P. Nordlander, and N. J. Halas, Coherent Fano resonances in a plasmonic nanocluster enhance optical four-wave mixing, *Proc. Natl. Acad. Sci. USA* **110**, 9215 (2013).
- [41] E. Poutrina, C. Ciraci, D. J. Gauthier, and D. R. Smith, Enhancing four-wave-mixing processes by nanowire arrays coupled to a gold film, *Opt. Express* **20**, 11005 (2012).
- [42] S. Panaro, A. Nazir, C. Liberale, G. Das, H. Wang, F. De Angelis, R. P. Zaccaria, E. Di Fabrizio, and A. Toma, Dark to bright mode conversion on dipolar nanoantennas: A symmetry-breaking approach, *ACS Photonics* **1**, 310 (2014).
- [43] P. Anger, P. Bharadwaj, and L. Novotny, Enhancement and Quenching of Single-Molecule Fluorescence, *Phys. Rev. Lett.* **96**, 113002 (2006).
- [44] B. C. Yildiz, M. E. Tasgin, M. K. Abak, S. Coskun, H. E. Unalan, and A. Bek, Enhanced second harmonic generation from coupled asymmetric plasmonic metal nanostructures, *J. Opt.* **17**, 125005 (2015).
- [45] N. B. Grosse, J. Heckmann, and U. Woggon, Nonlinear Plasmon-Photon Interaction Resolved by k -Space Spectroscopy, *Phys. Rev. Lett.* **108**, 136802 (2012).
- [46] S. A. Maier and H. A. Atwater, Plasmonics: Localization and guiding of electromagnetic energy in metal/dielectric structures, *J. Appl. Phys.* **98**, 011101 (2005).
- [47] The enhancement/suppression effect, due to Fano resonances in the nonlinear spectrum, are also observed for two coupled plasmonic materials [13,17]. In this case, coupling of QE to other modes, i.e., Ω_1 and Ω_2 , cannot be neglected [44].
- [48] M. Gunendi, I. Tanyeli, G. B. Akguc, A. Bek, R. Turan, and O. Gulseren, Understanding the plasmonic properties of dewetting formed Ag nanoparticles for large area solar cell applications, *Opt. Express* **21**, 18344 (2013).
- [49] B. Min, E. Ostby, V. Sorger, E. Ulin-Avila, L. Yang, X. Zhang, and K. Vahala, High- Q surface-plasmon-polariton whispering-gallery microcavity, *Nature (London)* **457**, 455 (2009).
- [50] See Supplemental Material <http://link.aps.org/supplemental/10.1103/PhysRevB.93.035410> for the time evolution and steady-state equations.
- [51] S. E. Harris, J. E. Field, and A. Imamoglu, Nonlinear Optical Processes Using Electromagnetically Induced Transparency, *Phys. Rev. Lett.* **64**, 1107 (1990).
- [52] M. Fleischhauer, A. Imamoglu, and J. P. Marangos, Electromagnetically induced transparency: Optics in coherent media, *Rev. Mod. Phys.* **77**, 633 (2005).